PHYSICAL REVIEW B VOLUME 15, NUMBER 11 1 JUNE 1977

Coherent interactions of Kramers doublet systems with microwaves in zero static magnetic field*†‡

Clark E. Davoust, Clyde A. Hutchison Jr., Marvin D. Kemple,§ Hie-Joon Kim, and Yung-Tsai Yen‖
The Department of Chemistry and The Enrico Fermi Institute, The University of Chicago, Chicago, Illinois, 60637
(Received 2 August 1976)

We have made the first magnetic-resonance observations of the coherent interactions of Kramers-doublet ions with microwave radiation in zero external static magnetic field. We have studied (a) population reversals by pulses of resonant microwave power and by adiabatic passage through resonance, (b) nutation, (c) free-induction signals, and (d) spin echoes, for the ~ 2-GHz $|4,0\rangle \leftrightarrow |3,0\rangle$ transition of $^{143}Nd^{3+}$ in $LaCl_3$ single crystals in the temperature range ~ 1.4 to ~ 4.2°K. For crystals in which approximately 7.4×10^{-4}, 9.8×10^{-4}, and 27.1×10^{-4} of the La^{3+} ions were replaced by $^{143}Nd^{3+}$ we have found that (a) the echo envelopes are well fitted by an exponential function; (b) the two-pulse echo envelopes and the Carr, Purcell, Meiboom, and Gill echo envelopes yield approximately the same values of the coherence time T_2; (c) the values of T_1 are sufficiently long that they do not affect the measured values of T_2; (d) the values of T_2 are roughly inversely proportional to the concentrations; (e) the values of T_2 are independent of temperature; and (f) spectral diffusion does not affect the measured value of T_2. For more dilute crystals in which $\sim 1.1\times10^{-4}$ of the La^{3+} ions were replaced, there was striking increase in the value of T_2, measured by the Carr, Purcell, Meiboom, and Gill technique, over its value at the higher concentrations, that was much greater than that given by inverse concentration dependence. Also in these more dilute crystals the two-pulse echo envelopes were not exponential and spin-diffusion effects were important.

I. INTRODUCTION

A. System

Coherent interactions of collections of two state systems with microwave radiation have been extensively studied by magnetic-resonance methods in the presence of external static magnetic fields in the cases of donor electrons in silicon,[1] paramagnetic ions in crystals,[2-5] organic doublet-state radicals in solids,[6] and organic triplet-state molecules.[7] Such interactions, in the absence of any external static magnetic field have been investigated only in the case of organic molecules in states of triplet-spin multiplicity.[8-12] We report here our observations of such phenomena in the case of $^{143}Nd^{3+}$ ions dilutely substituted for La^{3+} ions in $LaCl_3$ crystals in zero external static magnetic field.

The point symmetry at the La^{3+} site in $LaCl_3$ is C_{3h}.[13] When Nd^{3+}, $4f^3$, is substituted for La^{3+} in this crystal, the $^4I_{9/2}$ ground manifold of states of the Nd^{3+} is separated in energy into five Kramers doublets,[14,15] only the lowest of which is significantly populated at liquid He temperatures, inasmuch as the next doublet is 115 cm^{-1} higher in wave number.[14,15] In zero external magnetic field the two states of the ground doublet are strictly degenerate for the case in which the nuclear spin I is equal to zero for the Nd^{3+} and the other ions in the crystal, in accordance with the Kramers theorem. $^{143}Nd^{3+}$ has nuclear spin $I=\frac{7}{2}$. Primarily under the influence of the $^{143}Nd^{3+}$-electron nucleus hyperfine interaction the $2(2I+1)=16$ states of $^{143}Nd^{3+}$ form seven doublets and two singlets in the absence of any external magnetic field.[16] The wave-number difference between the highest and the lowest of the nine levels is ~0.152 cm^{-1}.[17] Magnetic-dipole resonance transitions, in zero external static magnetic field, between various of these levels may be excited by microwave fields. These resonances range in frequency from ~1998 to ~4564 MHz.[17] This magnetic-resonance spectrum for zero external static magnetic field has been studied previously in our laboratory.[17] It is described by the spin Hamiltonian

$$\mathcal{H}^0 = AI_zS_z + B(I_xS_x + I_yS_y) + PI_z^2, S=\tfrac{1}{2}, \quad I=\tfrac{7}{2}. \quad (1)$$

The $\hat{z}$ axis is the $\hat{c}$ axis of the crystal, i.e., the threefold symmetry axis at the Nd^{3+} site. The least-squares best fit of (1) to the observed spectrum was given by the following values[17] of the parameters at 4.2°K:

$$\begin{aligned} |A-2P|/h &= 1272.55\ (0.30)\ \text{MHz}, \\ |B|/h &= 499.506\ (0.010)\ \text{MHz}, \\ P/h &= +0.26\ (0.15)\ \text{MHz}. \end{aligned} \quad (2)$$

The standard deviations are given in parentheses and the sign of P/A is given. At 1.4°K, $|A-2P|$ was larger by a factor ~1.0003 and $|B|$ was smaller by a factor ~1.0001.

The spin Hamiltonian (1) has as eigenstates only those mixtures of products $|M_S, M_I\rangle$ of eigenstates

of S_z and I_z which have the same value of the sum, $M_F \equiv M_S + M_I$. For $M_F = +(I-\frac{1}{2}), +(I-\frac{1}{2})-1, \ldots, +1, 0, -1, \ldots, -(I-\frac{1}{2})$, the corresponding eigenvalues are

$$-\tfrac{1}{4}A + P(M_F^2 + \tfrac{1}{4}) \pm \tfrac{1}{2}\{(A-2P)^2 M_F^2 + B^2[I(I+1) - M_F^2 + \tfrac{1}{4}]\}^{1/2} , \quad (3)$$

and for $M_F = \pm(I+\frac{1}{2})$ they are

$$-\tfrac{1}{4}A + P(M_F^2 + \tfrac{1}{4}) + \tfrac{1}{2}|M_F|(A-2P) . \quad (4)$$

M_F is thus a quantum number for this system but $F = I \pm S$ is not, because $A \neq B$ and $P \neq 0$ in (1). However, $F = 3$ or 4 serves as a convenient state label, and we denote the states associated with the upper and lower signs in (3) by $|4, M_F\rangle$ and $|3, M_F\rangle$, respectively.

The transition that is of interest in the present paper is the one that occurs between the pair of $M_F = 0$ singlet states given by

$$|4,0\rangle = (1/\sqrt{2})(|+\tfrac{1}{2}, -\tfrac{1}{2}\rangle + |-\tfrac{1}{2}, +\tfrac{1}{2}\rangle) ,$$
$$|3,0\rangle = (1/\sqrt{2})(|+\tfrac{1}{2}, -\tfrac{1}{2}\rangle - |-\tfrac{1}{2}, +\tfrac{1}{2}\rangle) , \quad (5)$$

in which on the left-hand side the states are designated by $|F, M_F\rangle$ and on the right-hand side by $|M_S, M_I\rangle$. The corresponding eigenvalues of (1), as given by (3) are $-\frac{1}{4}A + \frac{1}{4}P \pm 2B$ with energy difference $4B = 1998.024$ MHz at 4.2 °K.[17] The expectation value of magnetic moment, electronic, and nuclear, is zero for these states. Magnetic-dipole transitions are induced between these two states by an oscillating magnetic field with magnitude $H_1 \cos(\omega t)$ polarized parallel to the $\hat{z}$ axis. The interaction of the Nd^{3+} ions with this oscillating field is described by

$$\mathcal{H}^1 = (+g_{\parallel}|\mu_B|S_z - g_n|\mu_N|I_z)\vec{H}_1 \cos(\omega t) , \quad (6)$$

in which $g_{\parallel} = 3.9946$,[18] μ_B is the Bohr magneton, g_n is 0.314,[17] and μ_N is the nuclear magneton. The absorption line due to the transition in zero external static magnetic field between the two states, (5) is much narrower in frequency than the lines due to the other allowed magnetic-dipole transitions (i.e., ~0.5-MHz full width at half-maximum intensity compared with ~30 MHz for all others, the former figure being somewhat dependent on the Nd^{3+} concentration). This narrowness results from the fact that the expectation values of the magnetic dipole moment for these states are zero. Because of this, there is very small magnetic dipole-dipole interaction with other ions and nuclei. Because this absorption is so narrow, we can study the coherent interactions with microwaves by using relatively low microwave power, namely, $\lesssim 1$ W.

B. Formal description of coherent interactions

For the case of an oscillating field $\vec{H}_1(t)$ at a frequency near the resonance frequency ~1998 MHz of the $|4,0\rangle \leftrightarrow |3,0\rangle$ transition of the $^{143}Nd^{3+}$ in zero external static magnetic field, we may to a good approximation neglect the other seven doubly degenerate levels and consider that we are dealing with an ensemble of two-state systems. It is well known[19,20] that for any such collection of quantum-mechanical two-state systems, perturbed by an oscillating field, we may define a fictitious spin ${}^f\vec{S}$ with $S = \frac{1}{2}$, a fictitious magnetic moment ${}^f\vec{\mu}$, a fictitious gyromagnetic ratio ${}^f\gamma$, and a fictitious magnetic field, ${}^f\vec{H}$, such that the equation of motion of the system appears in the form

$$\frac{d\langle {}^f\vec{\mu}\rangle}{dt} = +{}^f\gamma \langle {}^f\vec{\mu}\rangle \times {}^f\vec{H} , \quad (7)$$

in which $\langle {}^f\vec{\mu}\rangle$ is the expectation value of the fictitious magnetic moment for the collection of fictitious spins. The fictitious three-space magnetic field vector ${}^f\vec{H}$ is simply related to the matrix, $\vec{\mathcal{H}}$ of the Hamiltonian $\mathcal{H} = \mathcal{H}^0 + \mathcal{H}^1$ [given in our case by (1) and (6)], in the two-dimensional state space of the fictitious spin, with basis composed of the two states between which the resonance occurs. The relation is in the present instance given by

$$\begin{aligned} {}^f\gamma {}^fH_\xi &= -(2/\hbar)\,\mathrm{Re}\mathcal{H}_{12} \\ &= -(1/\hbar)(g_{\parallel}|\beta_e| + g_n|\beta_n|)H_1 \cos\omega t , \\ {}^f\gamma {}^fH_\eta &= +(2/\hbar)\,\mathrm{Im}\mathcal{H}_{12} = 0 , \\ {}^f\gamma {}^fH_\zeta &= +(1/\hbar)(\mathcal{H}_{22} - \mathcal{H}_{11}) = -4B/\hbar , \end{aligned} \quad (8)$$

in which 1, 2 denote $|4,0\rangle$, $|3,0\rangle$, respectively, and ξ, η, ζ, denote vector components in the fictitious-three-dimensional space in which lie the vectors ${}^f\vec{\mu}$ and ${}^f\vec{H}$. The fictitious moment ${}^f\vec{\mu}$ is the Pauli spin operator $\vec{\sigma}$ and so its expectation value $\langle\vec{\sigma}\rangle$ is the polarization of the fictitious spin system. The third component $\langle\sigma_\zeta\rangle$ of this polarization is a measure of the relative populations of the two states between which the resonance occurs, and the perpendicular components, $\langle\sigma_\xi\rangle$ and $\langle\sigma_\eta\rangle$, describe the coupling of the system to the real oscillating field $\vec{H}_1$, i.e., in our case, to the microwave field. Relation (7), which describes the temporal behavior of these quantities has the same form as the classical equation for the Larmor precession. Therefore, although the states of our two-state system have zero-expectation value of magnetic moment and there is no static external magnetic field, we may nevertheless discuss the temporal changes of the populations of the two states of this system and its interactions with the microwave field, in language formally the same

as that which we conventionally employ for describing the magnetic resonances of systems with real magnetic moments in finite external magnetic fields.

We use this formalism to discuss the results of our experiments. We consider the two states, (5), with $M_F = 0$, to be the eigenstates of a fictitious spin operator ${}^f\vec{S}$. The fictitious field ${}^f\vec{H}$ given by (8) is seen to have a static component ${}^fH_\zeta$ in the fictitious three-dimensional space, given by ${}^f\gamma\,{}^fH_\zeta = -4B/\hbar$, and also a linearly polarized oscillating component ${}^fH_\xi$ normal to the static field. This linearly polarized component may be resolved, in the same manner as is customary for real space, into two oppositely rotating components, one of which is effective in the reorientation of the magnetic moment of the fictitious spins. If we take the zero of energy to be $-\frac{1}{4}A + \frac{1}{4}P$, then the Hamiltonian appears in the form

$$\mathcal{H} = -\hbar\,{}^f\gamma\,{}^fH_\zeta\,{}^fS_\zeta + (g_\parallel|\beta_e| + g_n|\beta_n|)\tfrac{1}{2}H_1({}^fS_\xi\cos\omega t + {}^fS_\eta\sin\omega t)\ . \tag{9}$$

This describes a spin system in a static magnetic field ${}^fH_\zeta$ plus a perpendicular rotating field ${}^f\vec{H}_1$. It therefore becomes clear from the foregoing considerations that in order to interchange the populations of the two states (5), by means of the coherent interaction of the $^{143}Nd^{3+}$ ions with the microwave field, it will be necessary to apply a pulse of microwave power of duration sufficient to reverse the expectation value $\langle {}^f\vec{\mu}\rangle$ of the fictitious magnetic moment.[21] We see from (7) and (9) that in the rotating frame in the fictitious three-dimensional space, $\langle {}^f\vec{\mu}\rangle$ rotates about ${}^f\vec{H}_1$ with angular frequency $(1/\hbar)(g_\parallel|\beta_e| + g_n|\beta_n|)\frac{1}{2}H_1$. The required pulse would therefore be of duration $2\pi\hbar/H_1(g_\parallel|\beta_e| + g_n|\beta_n|)$, if the magnitude of the linearly polarized microwave magnetic field used to induce the transition [see (6)] is H_1. [The numerical value of $\pi\hbar/(g_\parallel|\beta_e| + g_n|\beta_n|)$ is 0.8942×10^{-7} G sec.] In a similar manner it will be seen that if the frequency of the applied microwave field is swept through the resonance at a rate slow enough that the adiabatic passage condition[21]

$$\frac{d\,{}^fH_\zeta}{dt} \ll {}^f\gamma\,{}^f\vec{H}_1^2 \tag{10}$$

is met with respect to the static and rotating components of the fictitious field, we would also expect to observe an interchange of the populations of the two states. It will also be seen that if the coherent interactions of the $^{143}Nd^{3+}$ ions with the microwave field are to be maximized, the microwave pulse must be of duration sufficient to tip $\langle {}^f\vec{\mu}\rangle$ through angle $\frac{1}{2}\pi$ in the fictitious three-dimensional space.[21] The required pulse would thus be one-half as long as that mentioned just above. One therefore expects to find a maximum in the intensity of the microwave field generated by the $^{143}Nd^{3+}$ ions (maximum "free-induction-decay signal"[21]) after the termination of a pulse of length Δt, when $\Delta t = \pi\hbar/H_1(g_\parallel|\beta_e| + g_n|\beta_n|)$. If pulses of microwave power of various durations were applied to the $^{143}Nd^{3+}$ ions and the coupling to the microwave field (free-induction-decay signal) measured after each, it would be anticipated that this coupling would vary periodically with the length of the pulse, as a result of the nutation of $\langle {}^f\vec{\mu}\rangle$ in the fictitious three-dimensional space under the influence of the microwave field. If a pulse of length, $\pi\hbar/H_1(g_\parallel|\beta_e| + g_n|\beta_n|)$, were applied to the $^{143}Nd^{3+}$ ions, and then after the absence of microwave stimulation for a period τ, a second pulse of twice that length were applied, we would expect to observe a spontaneous emission of microwave radiation ("spin echo"[22,23]) polarized parallel to the $\hat{c}$ axis of the crystal because of the restoration of the phase coherence of the rotating components of the fictitious magnetic moments ${}^f\vec{\mu}$ at that time, as a result of the second pulse.

C. Previous studies

In addition to the previous study in our laboratory of the zero-field magnetic-resonance spectrum[17] of $^{143}Nd^{3+}$ ions dilutely substituted for La^{3+} ions in $LaCl_3$ crystals, we have also previously reported the results of measurements of spin-lattice relaxation times T_1 for this system.[24] T_1 was measured by monitoring the recovery of the $|4,0\rangle \leftrightarrow |3,0\rangle$ absorption intensity as a function of time following saturation by pulses of microwave power at the resonance frequency ~1998 MHz.

II. EXPERIMENTAL DETAILS

A block diagram of the zero-field microwave magnetic-resonance apparatus used for the study of the coherent interactions is shown in Fig. 1. Pulsing of the microwave power incident on the cavity was accomplished with a PIN modulator driven by transistor-transistor logic circuits. The 60-MHz superheterodyne-detection system was protected by a second PIN modulator operated out of phase by π with respect to the first. No effect on the signals was observed when the second PIN modulator was removed. The PIN modulators had a dynamic range 80 dB and a switching time 50 nsec.

For free-induction and spin-echo experiments, the magnetization of the sample with resultant coupling to the microwave field that occurred subsequent to the termination of a microwave power

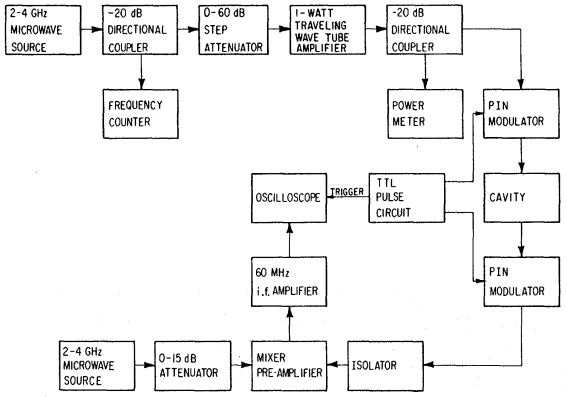

FIG. 1. Block diagram of zero-field microwave apparatus.

pulse, was detected by observing the 60-MHz signal from the IF amplifier with an oscilloscope that had a 50-MHz bandwidth. The response time of the complete detection system was ~0.2 μsec. Two-pulse spin-echo envelopes were obtained by varying the time between the two pulses, triggering the oscilloscope always at ~0.11 μsec before the beginning of the second pulse, and taking multiple-exposure photographs. Time markers were superimposed on the photographs to permit the determination of the times of appearance of the echoes. Care was taken to operate the detection system in its linear-response range.

The investigations of echoes generated by microwave pulse trains of the Carr and Purcell[25] and Meiboom and Gill[26] type were made by using hybrid junctions to divide the microwave power into two channels and to recombine them into a single channel again before reaching the traveling-wave tube amplifier. One channel contained a phase shifter of the trombone type followed by a PIN modulator, and the other contained a variable attenuator followed by a PIN modulator; the two PIN modulators shown in Fig. 1 were removed.

For the studies of nutation and reversal of level populations by adiabatic passage, during which it was desired to monitor the magnetic resonance absorption at low-incident microwave power after the termination of an excitation pulse, the apparatus shown in Fig. 1 was modified by insertion of a hybrid junction between the first PIN modulator and the cavity to allow for the introduction of ~10^{-8}-W monitoring power. In these cases the 60-MHz signal was detected with a diode detector and displayed on a signal averager. The linewidth measurements described below were made in this same manner. In all cases in which sequences of single or two-pulse experiments were made, a time at least equal to 10 times the measured spin-lattice relaxation time elapsed between the initiations of the successive experiments.

The single-crystal samples were placed in the cavity with the linearly polarized microwave magnetic field parallel to the $\hat{c}$ axis. The cavity was immersed in liquid He; and liquid He was in direct contact with the crystal sample. The cavity was of the reentrant type used previously in our laboratory[17] but with a smaller tuning range, namely, ~40 MHz. This smaller tuning range resulted from a change in design of the tuning mechanism which provided smoother tuning and better frequency stability. Measured Q values of the cavity containing the various crystal samples were in the range 350–450. The maximum amplitude of the linearly polarized microwave magnetic field at the sample may be crudely estimated from the cavity geometry to be ~1.2 G when 1 W of microwave power is dissipated in the cavity and $Q = 400$. The power incident on the first PIN modulator was monitored with a thermistor bridge power meter as indicated in Fig. 1. Power-meter readings given in later sections of this paper are the actual readings times 100 (–20-dB directional coupler). Measurements of power reflected from and transmitted by the cavity indicated that the power dissipated in the cavity was proportional to the power-meter reading and was equal to the fraction ~0.20 of the power incident on the first PIN modulator.

The vapor pressure of the liquid He in which the cavity was immersed was measured with a Bourdon pressure gauge or an oil manometer. From this pressure the temperature was determined to ~0.01°K by the use of the 1958 ^{4}He-vapor pressure scale of temperature.[27] The temperature was controlled to ~0.01°K by regulating the pressure.

The static magnetic field at the sample was reduced to $\lesssim 5$ mG by controlling the current in two sets of Helmholtz coils, with orthogonal axes, that were external to the cryostat. Another pair of external coils was used to apply a static field with magnitude ~40 G to the sample when it was desired to take the transition out of resonance in order (a) to verify the presence of a magnetic-resonance signal, (b) to establish a base line for the quantitative recording of a signal, or (c) to permit the determination of the response time of the detection system.

$LaCl_3$ single crystals with Nd^{3+} dilutely substituted for La^{3+} were prepared by the method of Anderson and Hutchison.[28] La_2O_3 from the Johnson Matthey Corp., and Nd_2O_3 enriched in ^{143}Nd and supplied by Oak Ridge National Laboratory, were used as starting materials. Crystal samples from four different $LaCl_3$ boules were used for the magnetic resonance experiments. These four boules are described in Table I. The crystal samples

TABLE I. Crystals used in the experiments. $LaCl_3$ with $^{143}Nd^{3+}$ dilutely substituted for La^{3+}. (Standard deviations are given in parentheses.)

Boule number	Fraction of La^{3+} sites occupied by $^{143}Nd^{3+}$. Calc. from composition of melt	Ratio of conc. of $^{143}Nd^{3+}$ in crystal to conc. of $^{143}Nd^{3+}$ in crystal sample number 2_1		
		Calc. from composition of melt	High-field EPR signal Intensity ratio	Crystal sample number
1	1.14×10^{-4} (9)	1.000 •••	1.000 •••	2_1
2[a]	7.4×10^{-4} (2)	6.5 (5)	9.1 (1.4)	2_2
3	9.8×10^{-4} (2)	8.6 (7)	13 (3)	5_3
4	27.1×10^{-4} (2)	24 (2)	48 (20)	1_4

[a] Boule 2 contained added Gd^{3+}. The fraction of La^{3+} sites occupied by Gd^{3+} was 0.270×10^{-4} (0.007) as calculated from the composition of the melts.

taken from these boules for the measurements were approximately 2mm×3mm×6mm in dimensions.

III. EXPERIMENTAL RESULTS

A. Interchange of populations

1. Microwave power pulses

The magnetic-resonance absorption intensity as a function of time, at 1.34°K, following the termination of a pulse of 1998.02-MHz microwave power with duration 1.1 μsec is shown as an oscilloscope trace in Fig. 2. The power-meter reading (see Sec. II and Fig. 1) was ~339 mW. The monitoring began ~0.1 msec after the termination of the pulse. The horizontal trace is the zero-signal base line, established in the manner described in Sec. II. The negative region of the absorption signal scale represents stimulated emission from the sample. A crystal sample from boule 2 (see Table I) was used.

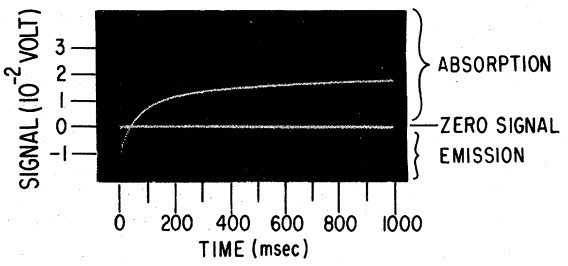

FIG. 2. Oscilloscope trace of magnetic resonance absorption intensity vs time following the termination of a pulse of microwave power. Microwave frequency 1998.02 MHz. Duration of pulse 1.1 μsec. Temperature 1.34°K. Crystal from boule 2 (see Table I).

The results of a sequence of experiments of the type described immediately above, in which the duration of the pulse was varied from experiment to experiment, are presented in Fig. 3. In this figure, the difference between the intensity of the wholly recovered absorption signal, and the intensity immediately after the termination of the pulse, (emission is negative intensity) is plotted versus the length of the pulse. The same sample and same temperature were used as for the experiment described in Fig. 2. The power-meter reading was ~170 mW. The $1/e$ time for the envelope of the maxima of Fig. 3 is 2.5 μsec with standard deviation 0.1 μsec.

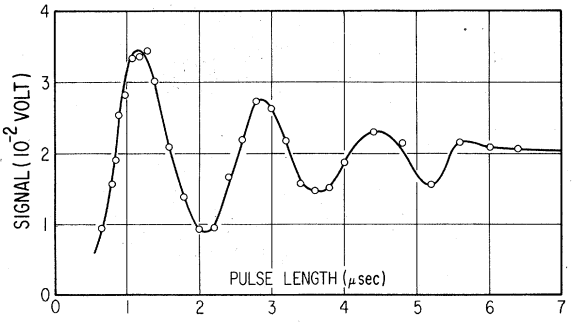

FIG. 3. Intensity of the wholly recovered absorption signal minus the intensity immediately after the termination of a pulse of microwave power plotted vs the duration of the pulse. Microwave frequency 1998.02 MHz. Temperature 1.34°K. Crystal from boule 2 (see Table I).

2. Adiabatic passage

In another set of experiments, the uninterrupted microwave power was swept in frequency and passed through the resonance line in ~10 μsec. Monitoring of the resonance absorption intensity began ~0.1 msec after this passage. A crystal from boule 3 (see Table I) was used. The results are shown as oscilloscope traces in Fig. 4 for experiments at 4.210 °K and 1.31 °K in which the resonance absorption was observed as a function of time after the termination of the passage.

B. Free-induction signals

The oscillating magnetizations of the sample at 4.21 °K, with resultant couplings to the microwave field and spontaneous generations of microwave radiation (free induction signals) that occurred subsequent to the termination of single pulses of microwave power at frequency 1998.02 MHz are shown as oscilloscope traces in Figs. 5(a), 5(b), 5(c), and 5(d). These traces were obtained as described in Sec. II. The power-meter reading was 339 mW (see Sec. II and Fig. 1). The length 0.84 μsec of the pulse used to obtain the trace in Fig. 5(b) was selected by means of a two-pulse echo experiment of the type described below in Sec. III D 1. It was set equal to the length of the first pulse of a $\frac{3}{2}\pi, 3\pi$ two-pulse sequence as defined below, and this length is designated as $t_{3\pi/2}$. The pulse lengths for Figs. 5(a), 5(c), and 5(d) were set at $\frac{1}{3}$, $\frac{5}{3}$, and $\frac{7}{3}$, respectively, times 0.84 μsec. These pulse lengths are designated as $t_{\pi/2}$, $t_{5\pi/2}$, and $t_{7\pi/2}$. In other experiments it was verified that pulses with lengths, $t_{\pi/2}$, $t_{3\pi/2}$, $t_{5\pi/2}$, and $t_{7\pi/2}$, produced local maxima in the intensity of the microwave radiation generated after the termination of the pulse, as the lengths of the pulses were varied in the vicinities of these values. Single pulses with lengths midway between those of the $\frac{1}{2}(2n+1)\pi$, $n=0, 1, 2, \ldots$ pulses just described are designated as $n\pi$ pulses, and the free-induction signals were nil after such pulses. The measurements of the durations of the single pulses that produced local maxima of intensity of the free-induction signals thus afforded a means of assigning the pulse designations, $\frac{1}{2}(2n+1)\pi$ and $n\pi$, $n=0, 1, 2, \ldots$ that agreed with the echo results described below, to within the fraction 0.03 of the pulse length.

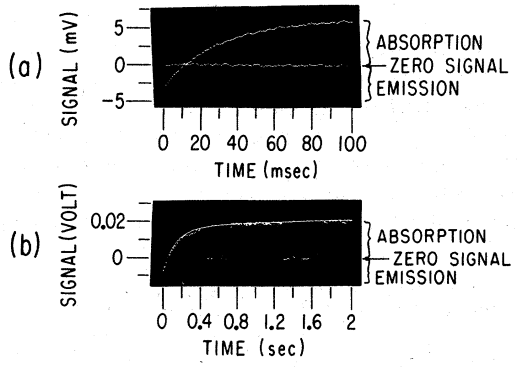

FIG. 4. Oscilloscope trace of magnetic resonance absoprtion intensity vs time following the adiabatic passage of the frequency of the microwave power through resonance. Crystal from boule 3 (see Table I). Temperature (a) 4.210 °K, (b) 1.31 °K.

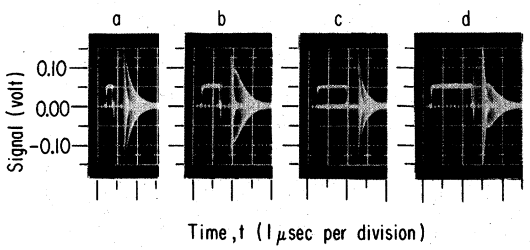

FIG. 5. Oscilloscope traces of intensities of microwave radiation generated by crystal after termination of single pulses of microwave power vs time. Microwave frequency 1998.02 MHz. Temperature 4.21 °K. Crystal from boule 2 (see Table I). Pulse: a, $\frac{1}{2}\pi$; b, $\frac{3}{2}\pi$; c, $\frac{5}{2}\pi$; d, $\frac{7}{2}\pi$.

For each of the four traces shown in Fig. 5, proceeding from the left, the first rectangular portion is a trace of the power pulse. It is followed by a 60-MHz envelope (see Sec. II) representing the relaxation of the disturbance of the detection system produced by the pulse. The last 60-MHz envelope is produced by the free-induction signal and shows its decay with time. The observation of the free-induction signal began ~0.6 μsec after the termination of the power pulse. A crystal from boule 2 (see Table I) was used for these experiments.

Similar experiments were performed with one crystal from boule 1, one crystal from boule 3, and one crystal from boule 4, and the results are summarized in Table II.

Experiments at 4.21 °K of the type just described, were done in which the power of the microwave pulse was varied. For each power level, a sequence of experiments was performed with pulse lengths $\frac{1}{3}(4n+3)$ times as large as the value of $t_{3\pi/2}(n=0, 1, 2, \ldots)$. Crystals from boules 1 and 3 (see Table I) were used for these experiments. The results concerning the power dependence of the fall-off of successive free-induction-decay maxima are summarized in Table III. For the first four rows of this table, $n=0, 1, 2, 3, 4$, and for the last two rows, $n=0, 1, 2, 3$.

TABLE II. $\Delta\nu_{1/2}$ full linewidth of EPR absorption at half-maximum intensity; $T_2^* \equiv 1/\pi\Delta\nu_{1/2}$; T_2^{FID}, $1/e$ time for free-induction decay after $\frac{1}{2}\pi$ pulse; and T_1, time constant for spin-lattice relaxation; for the $|4, 0\rangle \leftrightarrow |3, 0\rangle$ transition of $^{143}Nd^{3+}$ in $LaCl_3$ crystals in zero external static magnetic field.

Fraction of [a] La^{3+} sites occupied by $^{143}Nd^{3+}$	Linewidth measurement				Free-induction decay			Recovery from 4.3 sec pulse saturation		
	Crystal sample number (subscript is boule number [a])	Temp. of crystal (°K)	$\Delta\nu_{1/2}$ (MHz)	T_2^* (10^{-6} sec)	Crystal sample number (subscript is boule number [a])	Temp. of crystal (°K)	T_2^{FID} (10^{-6} sec)	Crystal sample number (subscript is boule number [a])	Temp. of crystal (°K)	T_1 (10^{-6} sec)
1.14×10^{-4} (9)	4_1	4.20 (1)	0.37 (1)	0.86 (3)	3_1	4.23 (1)	0.96 (1)	4_1	4.20 (1)	5.0×10^{4} [b] (1)
9.8×10^{-4} (2)	7_3	4.19 (1)	0.40 (1)	0.80 (2)	1_3	4.22 (1)	0.62 (1)	6_3	4.21 (1)	2.72×10^{4} [c] (5)
27.1×10^{-4} (2)	2_4	4.21 (1)	0.90 (4)	0.35 (2)	1_4	4.22 (1)	0.30 (7)	2_4	4.21 (1)	2.2×10^{4} [c] (1)

[a] See Table I.
[b] Reported in Ref. 24.
[c] Data from experiments of the type described in Sec. I C but not reported in Ref. 24.

It is of interest to note that the free induction signals following $\frac{1}{2}(4n+3)\pi$ pulses with $n=1, 2, \ldots$ increased for a period of time after observation was begun and before their subsequent decay, whereas for $\frac{1}{2}(4n+1)\pi$ pulses, only a decay was observed.

C. Linewidths

The full widths, in frequency, at half-maximum, of the absorptions by the $|4,0\rangle \leftrightarrow |3,0\rangle$ transition at 4.22°K of the $^{143}Nd^{3+}$ in boules 1, 3, and 4 (see Table I), were measured by low-power monitoring of the recovery of the magnetic resonance absorption after a saturating pulse of microwave power. A succession of such experiments over a range of microwave frequencies that spanned the absorption line of a given crystal, in which the magnitudes of the recovered signals were measured, gave an accurate determination of the line shape and linewidth. The results are given in Table II.

D. Spin echoes

1. Two-pulse echoes

Experiments were performed by the methods described in Sec. II in which two successive pulses of microwave power at frequencies 1998.02 MHz at ~4.2°K and 1997.94 MHz at ~2.3°K and ~1.4°K, were applied with an elapsed period τ between the termination of the first pulse and the beginning of the second. A spontaneous magnetization with resultant generation of microwave fields in the cavity (spin echo) was detected as described in Sec. II. The maximum of this echo occurred at a time interval $\tau + \sim 0.6$ μsec for $\frac{1}{2}\pi$; $\frac{5}{2}\pi$, 5π; and $\frac{2}{3}\pi$, $\frac{2}{3}\pi$ pulse pairs and $\tau + \sim 0.2$ μsec for a $\frac{3}{2}\pi, 3\pi$ pulse pair, after the termination of the second pulse. A sequence of such experiments was performed in which (a) the duration of the pulses was varied, (b) the second pulse was always just twice as long as the first, and (c) the interval τ was constant. Local maxima of the intensities of the spin echoes were observed as the lengths of the microwave power pulses were varied. The pulses of shortest duration that produced a local echo maximum are designated a $\frac{1}{2}\pi, \pi$ pulse pair. Pulses with lengths $2n+1$, $n=1, 2, \ldots$, times greater also produced similar local maxima. Such pulses are in general designated as $\frac{1}{2}(2n+1)\pi$, $(2n+1)\pi$, $n=0, 1, 2, \ldots$, pulse pairs. In a sequence of similar experiments in which the two pulses were of equal duration, the maximum echo amplitude occurred for a pulse length that was $\frac{4}{3}n$, $n=1, 2, 4, 5, 7, \ldots$, times as long as the first member of a $\frac{1}{2}\pi\pi$ pulse pair. A pulse of this length is designated a $\frac{2}{3}n\pi$ pulse.

TABLE III. Free-induction signal from $|4, 0\rangle \leftrightarrow |3, 0\rangle$ transition of $^{143}Nd^{3+}$ in $LaCl_3$ crystals at 4.21°K in zero external static magnetic field. Power dependence of time constant T_f for decrease of signal intensity with increase of pulse length for $\frac{1}{2}(4n+3)$ microwave pulses ($n=0, 1, 2, \ldots$). (Standard deviations are given in parentheses.)

Fraction of[a] La^{3+} sites occupied by $^{143}Nd^{3+}$	Crystal sample number (subscript is boule number)	Power-meter reading (mW)	T_f (10^{-6} sec)	$t_{3\pi/2}$, length of $\frac{3}{2}\pi$ pulse (10^{-6} sec)	$T_f/t_{3\pi/2}$
1.14×10^{-4} (9)	3_1	339	2.8 (1)	0.85 (1)	3.3 (1)
		107	4.8 (2)	1.39 (1)	3.5 (1)
		34	8.2 (5)	2.18 (1)	3.8 (2)
9.8×10^{-4} (2)	1_3	339	1.9 (1)	0.93 (1)	2.0 (1)
		107	2.7 (2)	1.34 (1)	2.0 (1)
		34	4.3 (4)	2.01 (1)	2.1 (2)

[a] From Table I.

In a sequence of such two-pulse echo experiments in which the lengths of both pulses were fixed but the interval τ between the termination of the first pulse and the initiation of the second pulse was varied, the maximum amplitude of the echo was observed to decrease as τ increased. The results of two such sequences of experiments are presented as photographs of oscilloscope traces in Figs. 6 and 7. These figures were obtained by the multiple exposure technique described in Sec. II. Each echo was recorded as a 60-MHz envelope in a separate exposure. The zero of the time scale is the time of triggering the oscilloscope which was ~0.11 μsec before the initiation of the second pulse. These figures were obtained for microwave frequency 1998.02 MHz and $\frac{1}{2}\pi, \pi$ pairs. Figure 6 was obtained at 4.22°K for a crystal from boule 2 (see Table I). Figure 7 was obtained at 4.21°K for a crystal from boule 1 (see Table I).

The results of 157 such sequences of two-pulse echo experiments are summarized in Table IV. Two different crystals from boule 2, five crystals from boule 3, and one crystal from boule 4 (see Table I) were used in these experiments. In addition, 38 such sequences of two-pulse echo experiments at 4.21 and 1.36°K were done with two crystals from boule 1 (see Table I) and those results are discussed below.

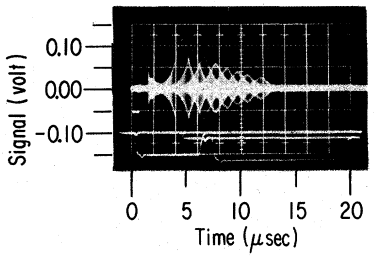

FIG. 6. Multiple-exposure photograph of oscilloscope traces of intensities of microwave echoes generated by crystal, following $\frac{1}{2}\pi, \pi$ pulse pairs of microwave power with varying intervals τ vs time. (The oscilloscope was triggered ~0.11 μsec before the initiation of the second pulse.) Microwave frequency 1998.02 MHz. Temperature 4.22°K. Crystal from boule 2 (see Table I).

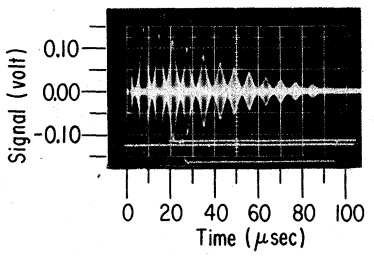

FIG. 7. Multiple-exposure photograph of oscilloscope traces of intensities of microwave echoes generated by crystal, following $\frac{1}{2}\pi, \pi$ pulse pairs of microwave power with varying intervals τ vs time. (The oscilloscope was triggered ~0.11 μsec before the initiation of the second pulse.) Microwave frequency 1998.02 MHz. Temperature 4.21°K. Crystal from boule 1 (see Table I).

TABLE IV. Summary of measurements of time constant T_2 for echo envelope for $|4, 0\rangle \leftrightarrow |3, 0\rangle$ transition of $^{143}Nd^{3+}$ in $LaCl_3$ crystals in zero external static magnetic field by the two-pulse method. (Standard deviations are given in parentheses.)

Fraction of [a] La^{3+} sites occupied by $^{143}Nd^{3+}$	Temp. of crystal (°K)	Crystal sample number (subscript is boule number[a])	T_2 (10^{-6} sec)	Power-meter reading (mW) 339 — Number of experiments with given pulse sequence and length, $t_{\pi/2}$, of $\frac{1}{2}\pi$ pulse (10^{-6} sec) $\frac{1}{2}\pi, \pi$	$\frac{3}{2}\pi, 3\pi$	$\frac{5}{2}\pi, 5\pi$	$\frac{2}{3}\pi, \frac{2}{3}\pi$	$t_{\pi/2}$	57 — $\frac{1}{2}\pi, \pi$	$t_{\pi/2}$	34 — $\frac{1}{2}\pi, \pi$	$t_{\pi/2}$
7.4×10^{-4} (2)	4.21 (1)	1_2	9.32 (30)	2	2	0	2	0.29 (1)	3	0.48 (2)	2	0.68 (2)
		2_2	9.76 (19)	1	0	0	0	0.28 (1)	0	•••	0	•••
	1.37 (1)	1_2	9.25 (39)	2	2	0	1	0.35 (1)	2	0.56 (1)	2	0.80 (1)
9.8×10^{-4}	4.21 (1)	1_3	6.04 (38)	11	16	6	6	0.30 (2)	11	0.47 (2)	9	0.68 (4)
		2_3	6.32 (1)	2	0	0	0	0.30 (3)	2	0.47 (1)	0	•••
		3_3	3.77 (6)	1	0	0	0	0.35 (1)	0	•••	0	•••
		4_3	3.20 (8)	1	0	0	0	0.33 (1)	0	•••	0	•••
		5_3	4.62 (51)	5	2	1	2	0.29 (7)	2	0.59 (1)	2	0.79 (2)
	2.43 (1)	1_3	6.41 (13)	6	0	0	0	0.32 (2)	8	0.52 (5)	6	0.72 (2)
	1.38 (2)	1_3	6.39 (20)	7	4	7	4	0.32 (1)	6	0.51 (4)	6	0.69 (5)
27.1×10^{-4} (2)	4.21 (1)	1_4	2.51 (9)	2	0	0	0	0.28 (1)	0	•••	0	•••
	1.38 (1)	1_4	2.32 (8)	1	0	0	0	0.46 (1)	0	•••	0	•••

[a] See Table I.

2. *Pulse-train echoes*

An example of the echoes obtained by the Carr, Purcell, Meiboom, and Gill technique (see Sec. II) at 4.21°K with microwave frequency 1998.02 MHz is shown as an oscilloscope trace in Fig. 8. A crystal from boule 1 (see Table I) was used for this experiment. The initial pulse was a $\frac{1}{2}\pi$ pulse with duration 0.95 μsec. It was followed by a sequence of π pulses of duration 1.91 μsec shifted in phase by $\frac{1}{2}\pi$ from the first pulse. τ, the period between the trailing edge of the $\frac{1}{2}\pi$ pulse and the leading edge of the first π pulse, was 9.6 μsec. The trailing edge of each π pulse was separated from the leading edge of the next π pulse in the sequence by an interval $2\tau = 19.2$ μsec. The zero of the time scale is the time of triggering the oscilloscope which was ~0.11 μsec before the initiation of the $\frac{1}{2}\pi$ pulse. The displayed 60-MHz envelopes are the successive echo signals. For experiments at 1.36°K the microwave frequency was 1997.94 MHz.

The results of 40 such Carr, Purcell, Meiboom, and Gill echo experiments are summarized in Table V. Two different crystals from boule 1, one crystal from boule 2, and two crystals from boule 3 (see Table I) were used in these experiments.

It was observed that for a given crystal sample from boule 1 (see Table I) the $1/e$ time for decay of the echo envelope was constant for $\sim 5 \leq \tau \leq \sim 10$ μsec. The experiments with τ in this range are summarized in Table V. As the value of τ was increased in the range from 20 to 50 μsec, the $1/e$

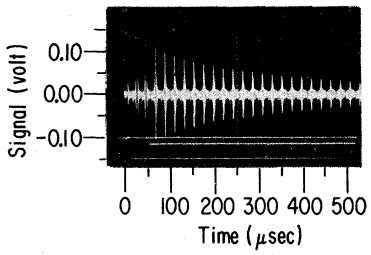

FIG. 8. Oscilloscope trace of intensities of microwave echoes generated by crystal following the pulses of a Carr, Purcell, Meiboom, and Gill sequence vs time. (The oscilloscope was triggered at the beginning of the first pulse.) Microwave frequency 1998.02 MHz. Pulse interval 9.6 μsec. Temperature 4.21 °K. Crystal from boule 1 (see Table I).

time decreased, typically, to $\sim\frac{2}{3}$ of its value at the shorter τ's.

IV. DISCUSSION OF RESULTS

A. Interchange of populations

Figure 2 (see Sec. III A 1) clearly demonstrates that a pulse of microwave power produces in this two-state system a population reversal of the type discussed in Sec. I B. The return of the magnetic resonance absorption signal intensity, with its associated relative populations of the two states, to its thermal equilibrium value does not begin from the zero-signal level. Thus, this pulse did not produce just a saturated signal with equalized populations. The sequence of such experiments summarized in Fig. 3 demonstrates those coherent interactions of the two-state $^{143}Nd^{3+}$ system, with microwaves (in zero external static magnetic field), which may be formally described, in accordance with Eq. (7), as the nutation of the expectation value $\langle {}^f\vec{\mu}\rangle$ of the fictitious moment ${}^f\vec{\mu}$ (defined in Sec. I B), in the fictitious field ${}^f\vec{H}$. ${}^f\vec{H}$ has the static component ${}^fH_\zeta$ along the fictitious ζ axis, given by ${}^f\gamma\,{}^fH_\zeta = -4B/\hbar$ [see Eqs. (8)] and the oscillating component ${}^fH_\xi$ (normal to ${}^fH_\zeta$) given by ${}^f\gamma\,{}^fH_\xi = -(1/\hbar)(g_\parallel|\beta_e| + g_n|\beta_n|)H_1\cos\omega t$ [see Eqs. (8)] in which H_1 is the amplitude of the applied microwave field. Thus (see Sec. I B) as $\langle {}^f\vec{\mu}\rangle$ nutates its direction is reversed in a period

$$2\pi\hbar/H_1(g_\parallel|\beta_e| + g_n|\beta_n|) = 2\times 0.894\times 10^{-7}H_1^{-1}\ \text{sec}\ ,$$

if H_1 is given in G. $\langle {}^f\vec{\mu}\rangle$ measures the relative populations of the two states $|4,0\rangle$ and $|3,0\rangle$, which are seen to be interchanged in this same period. From the crude estimate of the value of H_1 in the cavity, given in Sec. II, based on the power-meter reading, we see that for this sequence of experiments, $H_1 \cong 0.22$ G and so the reversal period for $\langle {}^f\vec{\mu}\rangle$ is ~0.8 μsec. From Fig. 3, one sees that the mean time for the four reversals immediately following the first one (the first one is neglected because of some experimental uncertainty as to the origin of the time scale) is ~0.8 μsec, in rough agreement with the estimated microwave magnetic field strength.

It is seen from Fig. 3 that as the pulse length in-

TABLE V. Summary of measurements of time constant T_2 for echo envelope for $|4,0\rangle \leftrightarrow |3,0\rangle$ transition of $^{143}Nd^{3+}$ in $LaCl_3$ crystals in zero external static magnetic field by the Carr, Purcell, Meiboom, Gill method. (Standard deviations are given in parentheses.)

Fraction of [a] La^{3+} sites occupied by $^{143}Nd^{3+}$	Temp. of crystal (°K)	Crystal sample number (subscript is boule number[a])	T_2 (10^{-6} sec)	Number of experiments	Range of τ values (10^{-6} sec)	Range of $t_{\pi/2}$ values (10^{-6} sec)
1.14×10^{-4} (9)	4.21 (1)	1_1	363 (25)	5	4.7 – 18.9 (1) (2)	1.00 – 1.29 (2) (2)
		1_1 and 2_1	352 (23)	22	5.1 – 19.5 (1) (2)	0.59 – 1.54 (1) (2)
	1.36 (1)	1_1 and 2_1	346 (1)	2	9.7 – 9.8 (1) (1)	0.78 – 0.80 (1) (1)
7.4×10^{-4} (2)	4.20 (1)	2_2	8.7 (6)	5	2.4 – 4.7 (1) (1)	0.50 – 1.05 (1) (2)
9.8×10^{-4} (2)	4.21 (1)	3_3	3.89 (26)	1	1.79 (1)	0.38 (1)
		5_3	5.69 (32)	5	1.38 – 1.98 (1) (1)	0.58 – 0.67 (1) (1)

[a] See Table I.

creases, the amplitude of the oscillations of the intensity of the absorption signal immediately following the pulse decreases to zero. We show below that inhomogeneities in the microwave H_1 field over the volume of the sample constitute the dominant factor producing this decay.

The results presented in Fig. 4 (see Sec. III A) demonstrate population interchange by means of coherent interactions that may be described as an adiabatic passage of the fictitious field ${}^fH_\zeta$ through resonance at a rate slow enough to satisfy the adiabatic condition (10). This condition is seen to be equivalent to the statement that the ratio of the linewidth 0.40 MHz (see Table III), to the time ~10 μsec (see Sec. III A 2) required for the microwave frequency to be swept through the $|4,0\rangle \leftrightarrow |3,0\rangle$ absorption line, should be much smaller than the reciprocal of the square of $t_\pi \cong 0.60$ μsec (see Table IV), the time required for the reversal of the direction of the fictitious moment. This condition is certainly well satisfied.

B. Free-induction signals

Figure 5 and the results summarized in Table II, show that in zero external static magnetic field the $^{143}Nd^{3+}$ crystal samples generate microwave radiation (free-induction signals) after the termination of pulses of microwave power, as a result of their oscillating macroscopic magnetizations. In accordance with the discussion of Sec. I B, the coherent interactions of the fictitious spins with the microwave field at the resonance frequency for the $|4,0\rangle \leftrightarrow |3,0\rangle$ transition, and with strength H_1 will tilt the expectation value $\langle {}^f\vec{\mu}\rangle$ of the fictitious moment ${}^f\vec{\mu}$ through angles, $\frac{1}{2}(2n+1)\pi$, $n=0,\ 1,\ 2,\ldots$ in the fictitious-three-dimensional space, in periods

$$(2n+1)\pi\hbar/H_1(g_\parallel|\beta_e| + g_n|\beta_n|) \ .$$

As a result, the crystal sample will have a spontaneous oscillating magnetization that is a maximum following microwave pulses with these durations. Estimates of the value of H_1, of the type made in Sec. IV A, show that the pulse lengths, observed to produce local maxima in the free-induction signal intensity, have the values expected on the basis of the considerations in Sec. I B.

The free-induction-decay envelopes were least-squares fitted by exponential functions and the $1/e$ time $T_2^{\rm FID}$ corresponding to these functions are given in Table II. For a cavity with $Q=400$ (see Sec. II) the $1/e$ time for the decay of the 1998 MHz stored energy in cavity field is 32 nsec. The cavity ringing is thus a negligible perturbation on these measured values of $T_2^{\rm FID}$. The values of T_1, the spin-lattice relaxation time, measured as described in Sec. I C, are also listed in Table II. They are clearly sufficiently large that they do not affect the measured values of $T_2^{\rm FID}$.

The values of the decay constants for the free induction signals are seen to display the expected direct correlation with the linewidths listed in Table II for the resonance absorptions. The values of $T_2^* \equiv 1/\pi\Delta\nu_{1/2}$, in which $\Delta\nu_{1/2}$ is the full width at half-maximum intensity, show the expected behavior as $T_2^{\rm FID}$ varies for the crystal of varying $^{143}Nd^{3+}$ ion concentration.

In Table III, are summarized the results of measurements of the intensities of the free-induction signals after single microwave pulses of various durations at various power levels. The values of the free-induction signal maxima, following $\frac{1}{2}(4n+3)\pi, n=0,\ 1,\ 2,\ldots$ pulses (see the last paragraph of Sec. III B) as a function of the lengths of the successive pulses, were least-squares fitted by an exponential function of the time. The $1/e$ times T_f, so obtained, for the fall-off of the intensities of successive free-induction signals, are listed. The observed decreasing values of T_f as the power of the $\frac{1}{2}(4n+3)\pi$ pulses is increased are directly proportional to the durations of the $\frac{3}{2}\pi$ pulses, and the constant ratio is listed in the last column of Table III. These results show very clearly that this fall-off is the result of inhomogeneity of the microwave magnetic field H_1 over the volume of the crystal. As a result of this inhomogeneity, the amplitudes of the population reversals, described as a nutation of $\langle {}^f\vec{\mu}\rangle$ in Secs. I B and IV A, should decay in a similar manner. It has already been pointed out that this is, in fact, the observed behavior. Thus the decrease in the nutation amplitude arises from this source rather than from some true T_2 process.

The occurrence of the maxima in the free-induction signals following $\frac{1}{2}(4n+3)\pi$ pulses will be discussed below.

C. Spin echoes

1. Two-pulse echoes

The results of the sequences of two-pulse echo experiments, described in the last two paragraphs of Sec. III D, for crystals from boules 2, 3, and 4 (see Table I), are summarized in Table IV. The individual sequences were all similar to those represented in Figs. 6 and 7 which are described in Sec. III D.1. These echo evelopes (maximum echo intensity versus time at which the maximum occurs) were least-squares fitted by an exponential function ae^{-2t/T_2} in which a and T_2 are adjustable constants and t is time, after initiation of the second pulse, at which the maximum of the echo occurred. T_2 so obtained for the decrease of the echo

amplitude with echo time, is listed as a function of temperature, power level, and crystal sample. The variations of T_2 for different crystals from the same boule are presumed to result from inhomogeneities in the distribution of the $^{143}Nd^{3+}$ ions throughout the boule. For crystals from boule 1, which contained the lowest concentration of $^{143}Nd^{3+}$ ions, the decrease of echo maximum intensity with time at which the echo occurred was not exponential. These experiments will be discussed below.

If the resonance absorption line is inhomogeneously broadened, then the decay time T_2 for the echo envelope should be longer than the $1/e$ time T_2^{FID} for the decay of the free-induction signal. Comparison of Tables II and IV show that this is indeed the case. The values of T_1, listed in Table II, are clearly sufficiently large that they do not affect the measured values of T_2.

The time T_2 is seen to be independent of power over the 10-dB range which we were able to study, independent of temperature between ~1.4 and ~4.2°K, and independent of the type of pulse pair used. However T_2 does show a marked dependence on concentration of the $^{143}Nd^{3+}$ ion. In fact T_2 is close to inversely proportional to the concentration of $^{143}Nd^{3+}$. It is also to be noted that in boule 2, 0.27×10^{-4} of the La^{3+} sites were occupied by Gd^{3+} ions and that this apparently does not strongly influence the value of T_2.

In Table VI the values of $g_{\parallel}|\beta_e|H_1/2\hbar = 1/(4t_{\pi/2})$ are compared, for crystals from boules 1 and 3 (see Table I) with the measured linewidths (see Table II) of their EPR absorption for the $|4,0\rangle \leftrightarrow |3,0\rangle$ transition. In each case τ was the interval between the $\frac{1}{2}\pi$ and π pulses for the first echo of the sequence. For boule 1, the 34 data at ~4.21°K from the 38 experiments mentioned in Sec. III D 1, were used, for 12 of which $\sim 5 < \tau < 7$ μsec and for 22 of which $\sim 24 < \tau < \sim 26$ μsec. The comparison is made for various power levels. It is clear that $g_{\parallel}|\beta_e|H_1/2\hbar \gtrsim$ linewidth. This fact, coupled with the observed lack of dependence of T_2 on the microwave power (see Table IV) shows that spectral diffusion plays no important role in determining the

TABLE VI. Comparison of $g_{\parallel}|\beta_e|H_1/h = 1/4t_{\pi/2}$ with the full linewidth $\Delta\nu_{1/2}$ at half-maximum intensity of the EPR absorption by the $|4, 0\rangle \leftrightarrow |3, 0\rangle$ transition of $^{143}Nd^{3+}$ in $LaCl_3$ crystals in zero external static magnetic field. (Standard deviations are given in parentheses.)

		$\frac{1}{2}\pi, \pi$ two-pulse echo experiments $\frac{g_{\parallel}\|\beta_e\|H_1}{2\hbar} = \frac{1}{4t_{\pi/2}}$ (MHz) For given power-meter reading			
Fraction of [a] La^{3+} sites occupied by $^{143}Nd^{3+}$	Crystal sample number (subscript is boule number [a])	Temp. of crystal (°K)	339 (mW)	107 (mW)	34 (mW)	$\Delta\nu_{1/2}$ [c] (MHz)
1.14×10^{-4} (9)	1_1	4.21 (1)	0.71 (2)	0.47 (1)	0.29 (1)	0.37 (1)
	3_1	4.21 (1)	0.71 (18)	0.47 (4)	0.34 (1)	
	5_1	4.21 (1)	0.73 (6)	0.43 (3)	0.28 (1)	
9.8×10^{-4} [b] (2)	1_3	4.21 (1)	0.83 (5)	0.53 (2)	0.37 (2)	0.40 (1)
	2_3	4.21 (1)	0.83 (3)	0.53 (2)	•••	
	3_3	4.20 (1)	0.71 (2)	•••	•••	
	4_3	4.22 (1)	0.76 (2)	•••	•••	
	5_3	4.20 (1)	0.86 (21)	0.42 (1)	0.32 (1)	

[a] See Table I.
[b] $t_{\pi/2}$ data from Table IV.
[c] Data from Table III.

measured values of T_2 for the crystal from boule 3. The microwave pulse does not "burn a hole" in the absorption line but rather is able to flip all fictitious spin packets of the inhomogeneously broadened line. As a result of this fact the fictitious effective field ${}^f\vec{H}_{\text{eff}}$ in the rotating frame in the fictitious three-dimensional space, makes an angle with ${}^f\vec{H}_1$ that is appreciably different from zero for a large fraction of the fictitious spin packets. This results in a spread in the directions (in the fictitious rotating axes) of the spin packets at the end of a $\frac{1}{2}(2n+1)\pi$ pulse that continues to increase subsequent to $\frac{1}{2}(4n+1)\pi, n=0, 1, 2, \ldots$ pulses. But after $\frac{1}{2}(4n+3)\pi$ pulses the spin packets are moving in such a direction that they refocus and then spread. As a result the associated oscillating component of the macroscopic magnetization produces the maximum in the free-induction signal some time after the cessation of the $\frac{1}{2}(4n+3)\pi$ pulses as seen in Fig. 5 and noted in Sec. III B, whereas only a decay is seen after the $\frac{1}{2}(4n+1)\pi$ pulses. This fact also accounts for the different echo occurrence time after $\frac{3}{2}\pi, 3\pi$ pulse pairs that was described at the beginning of Sec. III D.

It is to be noted that there is no modulation of the echo envelopes, by nuclear interactions, of the type observed in echo experiments with such crystals in external magnetic fields.[29]

2. *Pulse-train echoes*

The results of the Carr, Purcell, Meiboom, and Gill echo experiments, described in Sec. III D, for crystals from boules 1, 2, and 3 (see Table I) are summarized in Table V. The individual sequences were all similar to the one represented in Fig. 8. The intensities of the echo maxima versus the time at which they occurred were least-squares fitted with an exponential function ae^{-t/T_2} in which a and T_2 are adjustable constants and t is the time, after the termination of the first pulse, at which the maximum of the echo occurred. The $1/e$ times for the decay of the echo intensity are listed in Table V.

For crystals from boules 2 and 3, Tables IV and V show that there is approximate agreement between the values of T_2 obtained from the two-pulse echo envelopes and from the Carr, Purcell, Meiboom, and Gill experiments. The comparison can be best made for cases in which measurements were made by both methods on the same crystal samples, i.e., crystals 2_2, 3_3, and 5_3, thus eliminating the previously mentioned effects of inhomogeneity of concentration of $^{143}Nd^{3+}$ throughout the boule. For crystals from boule 1, however, the comparison cannot be made because, as mentioned in Sec. IV C 1, the two-pulse echo envelopes deviate strongly from exponential behavior, whereas the Carr, Purcell, Meiboom, and Gill envelopes for boule 1 crystals are well fitted by an exponential function except for the first three or four echoes. There is a strikingly large increase in the T_2 time obtained by the Carr, Purcell, Meiboom, and Gill technique on going from the next to lowest concentration (boule 2) crystals to the ones of lowest concentration, a change by a factor ~7–9 (see Table I).

On the supposition that (a) the observed nonexponentiality of the two-pulse echo envelopes for the most dilute crystals, and (b) the decrease in the apparent T_2 when for these same crystals the interval τ in the Carr, Purcell, Meiboom, and Gill experiment is increased, might both indicate the occurrence of spin diffusion processes, we least-squares fitted the functions

$$ae^{-[(2t/T_2)+mt^2]} \tag{11}$$

and

$$ae^{-[(2t/T_2)+mt^3]} \tag{12}$$

to each of 14 of the 38 two-pulse spin echo envelopes mentioned in Sec. III D 1. These 13 included all those for which the values of τ for the first echo of the envelope satisfied $\sim 5 < \tau < \sim 7$ μsec except for two in which the second pulses were shifted in phase by $\frac{1}{2}\pi$ with respect to the first. In these expressions a and m are adjustable constants, t is the time after the termination of the second pulse, and T_2 was taken to be the T_2 measured for the same crystal by the Carr, Purcell, Meiboom, and Gill method, and listed in Table V. On the basis of considerations of certain theoretical models, functions such as (11) and (12) have in the past been suggested as expected descriptions of the spin echo envelopes when the spin containing species was diffusing in a liquid,[25] or when spin was diffusing in a solid.[30,31] We suppose that in the case of these most dilute crystals, we are for the shortest τ's of the envelope, measuring the actual coherence time T_2 for the energy-conserving mutual fictitious spin-flip exchange of resonance energy among the $^{143}Nd^{3+}$ ions, whereas in the longer τ portion of the envelope, spin-diffusion processes have played an appreciable role, and produce a nonexponential behavior.

Figure 9 shows a typical least-squares fit of the function ae^{-2t/T_2} to a two-pulse spin-echo envelope as described in Sec. IV C 1 for the crystals of higher concentration. The results of such fits are listed in Table IV. The fit is seen to be very good. Fig. 10 illustrates a typical case of the lack of exponentiality for the two-pulse echo envelopes for the crystals most dilute in $^{143}Nd^{3+}$. Here the exponential function is clearly seen to give a poor

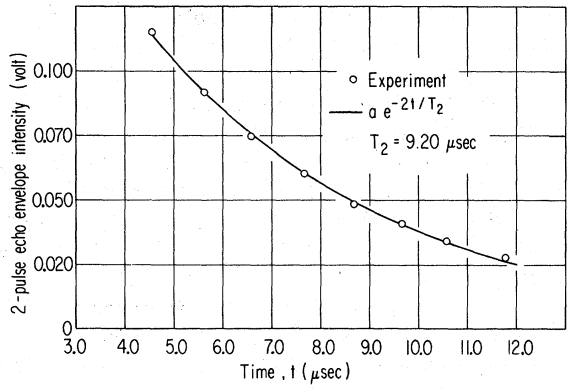

FIG. 9. Two-pulse echo envelope intensity vs time (from Fig. 6). The curve was obtained by least-squares fitting of ae^{-2t/T_2} to the plotted points by adjustment of a and T_2.

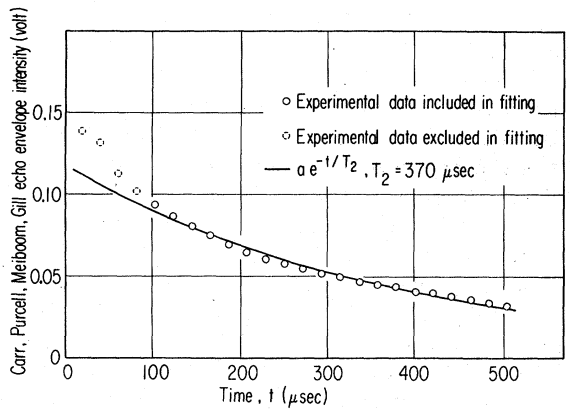

FIG. 11. Carr, Purcell, Meiboom, and Gill echo envelope intensity vs time (from Fig. 8). The curve was obtained by least-squares fitting of ae^{-t/T_2} to the plotted points by adjustment of a and T_2.

least-squares fit. The least-squares fits, to the same data, of the functions with quadratic and cubic terms are also shown in Fig. 10. The function with a quadratic term in the exponent is seen to give a much better fit than does the simple exponential. Figure 11 shows a typical least-squares fit of an exponential function to a Carr, Purcell, Meiboom, and Gill echo envelope, as described at the beginning of the present section, for crystals with the lowest concentration of $^{143}Nd^{3+}$. In this case, except for the first 4 times which were neglected in the fitting, the simple exponential function clearly gives a good fit, whereas from Fig. 10 it is clear that this is not the case for the two-pulse echo envelope. The first four echoes (up to 100 μsec) were neglected because of the same rephasing effects for the different fictitious spin packets as were mentioned at the end of Sec. IV C 1 in relation to the free-induction signals, and which

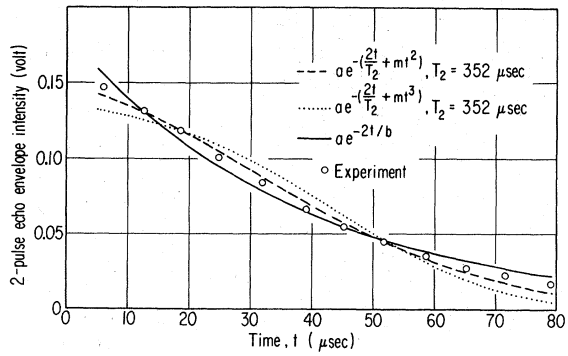

FIG. 10. Two-pulse echo envelope intensity vs time (from Fig. 7). The curves were obtained by least-squares fittings of the indicated functions to the plotted points by adjustment of a and m, or of a and b. T_2 was fixed at 352 μsec.

become quite apparent in the Carr, Purcell, Meiboom, and Gill envelopes for these most dilute crystals.

The least-squares fittings of (11) to the 13 envelopes by adjustment of the value of m gives a mean value 2.95×10^{-4} μsec^{-2} for m. The standard deviations of the m values for these least-squares fits range from 0.10×10^{-4} to 0.18×10^{-4} μsec^{-2} with average value 0.14×10^{-4} μsec^{-2}. The fitting with (12) yields the mean value 4.97×10^{-6} μsec^{-3} for m, and the standard deviations range from 0.52×10^{-6} to 0.77×10^{-6} μsec^{-3} with average value, 0.67×10^{-6} μsec^{-3}. The relatively good fit provided by (11) may be considered to support the above-mentioned interpretation of the nonexponential behavior of the envelopes and the possibility of treating the effects of fictitious spin diffusion for larger τ's in a manner formally identical with the treatment of the effects of matter diffusion in a liquid or spin diffusion in a solid in the case of actual spins. With this interpretation, the good fit of (11) to the envelopes may be said to demonstrate the fact that both the two-pulse and the Carr, Purcell, Meiboom, and Gill methods yield the same value for the "true" T_2 for this $^{143}Nd^{3+}$ system of fictitious spins, in these most dilute crystals as well as in the cases of the more concentrated crystals discussed at the beginning of this section. Equation (11) has been proposed for the case of Lorentzian diffusion,[30] and (12) for the case of Gaussian diffusion[31]; and (11) gives a somewhat better fit to our results. Of course, such effects may exist for the higher concentration crystals discussed above, but for these crystals the echo maxima decay with increasing value of τ due to T_2 before the quadratic term representing the diffusion effects has become appreciable.

V. SUMMARY

We have demonstrated that the coherent interactions of an ensemble of Kramers ions with microwave radiation in zero external static magnetic field can be observed. We have measured the coherence lifetime T_2 for the $|4,0\rangle \leftrightarrow |3,0\rangle$ transition of $^{143}Nd^{3+}$ in $LaCl_3$ single crystals. For crystals of the higher concentrations in which 7.4×10^{-4}, 9.8×10^{-4}, and 27.1×10^{-4} of the La^{3+} ions have been replaced by $^{143}Nd^{3+}$ we have found that (a) the echo envelopes are well fitted by an exponential function; (b) the two-pulse echo envelopes and the Carr, Purcell, Meiboom, and Gill echo envelopes yield the same values of T_2; (c) the values of T_1 are sufficiently long that they do not affect the measured values of T_2; (d) the values of T_2 are approximately inversely proportional to the $^{143}Nd^{3+}$ concentration; (e) the measured values of T_2 are independent of temperature in the range ~1.4 to ~4.2°K; and (f) spectral diffusion does not affect the measured values of T_2. For the lowest concentration crystal, in which only $\sim 1.1 \times 10^{-4}$ of the La^{3+} ions were replaced by $^{143}Nd^{3+}$, there is a striking increase in the value of T_2, measured by the method of Carr, Purcell, Meiboom, and Gill, over its value at the higher concentrations, that is much greater than that given by an inverse concentration dependence. Also in these most dilute crystals the two-pulse echo envelopes are not exponential and spin diffusion effects are important.

Interaction of the $^{143}Nd^{3+}$ ions with Cl and La nuclei in their vicinity is not a significant factor in the values of T_2 measured in these experiments. Magnetic dipolar interactions in zero external field between $^{143}Nd^{3+}$ ions in the states $|4,0\rangle$ and $|3,0\rangle$ and Cl and La nuclei are very greatly reduced from the values of the interactions in external fields of several thousand gauss because the expectation value of the magnetic dipole moment of $^{143}Nd^{3+}$ in these states is zero. It is presumably for this reason that no nuclear modulation of the spin echo envelopes was observed. Such modulation may be expected to be observed in the case of similar experiments employing other zero-field transitions between the hyperfine levels of $^{143}Nd^{3+}$ in $LaCl_3$. On the other hand the interactions between $^{143}Nd^{3+}$ ions are much larger and can be responsible for the observed values of T_2.

One of us (M.D.K.) expresses his thanks to the Enrico Fermi Institute of the University of Chicago for the award of the Enrico Fermi Fellowship for the year 1971–1972.

---

*Research supported by the NSF.
†Some equipment used in this work was supplied by the Advanced Research Projects Agency.
‡Supported in part by The Louis Block Fund, The University of Chicago.
§Present address: Physics B120, Natl. Bur. Stds. (U.S.), Washington, D. C. 20234.
||Present address: Dept. of Chemistry, National Taiwan University, Taipei, Taiwan, Republic of China.

[1]J. P. Gordon and K. D. Bowers, Phys. Rev. Lett. 1, 368 (1958).
[2]W. B. Mims, K. Nassau, and J. D. McGee, Phys. Rev. 123, 2059 (1961).
[3]J. A. Cowen and D. E. Kaplan, Phys. Rev. 124, 1098 (1961).
[4]W. B. Mims, Rev. Sci. Instrum. 36, 1472 (1965).
[5]W. B. Mims, Phys. Rev. 168, 370 (1968).
[6]I. M. Brown, J. Chem. Phys. 55, 2377 (1971).
[7]B. J. Botter, D. C. Doetschman, J. Schmidt, and J. H. van der Waals, Mol. Phys. 30, 609 (1975).
[8]J. Schmidt, Chem. Phys. Lett. 14, 411 (1972).
[9]C. A. van't Hof, J. Schmidt, P. J. F. Verbeek, and J. H. van der Waals, Chem. Phys. Lett. 21, 437 (1973).
[10]W. G. Breiland, C. B. Harris, and A. Pines, Phys. Rev. Lett. 30, 158 (1973).
[11]C. B. Harris, R. L. Schlupp, and H. Schuch, Phys. Rev. Lett. 30, 1019 (1973).
[12]W. G. Breiland, H. C. Brenner, and C. B. Harris, J. Chem. Phys. 62, 3458 (1975).
[13]W. H. Zachariasen, J. Chem. Phys. 16, 254 (1948).
[14]E. Carlson and G. H. Dieke, J. Chem. Phys. 29, 229 (1958).
[15]E. H. Carlson and G. H. Dieke, J. Chem. Phys. 34, 1602 (1961).
[16]B. Bleaney, Philos. Mag. xlii, 441 (1951).
[17]L. E. Erickson, Phys. Rev. 143, 295 (1966).
[18]J. P. Hessler and C. A. Hutchison Jr., Phys. Rev. B 8, 1822 (1973).
[19]R. P. Feynman, F. L. Vernon, Jr., and R. W. Hellwarth, J. Appl. Phys. 28, 49 (1957).
[20]A. Abragam, *The Principles of Nuclear Magnetism* (Oxford U. P., Oxford, 1961), p. 36.
[21]F. Bloch, Phys. Rev. 70, 460 (1946).
[22]E. L. Hahn, Phys. Rev. 80, 58 (1950).
[23]N. A. Kurnit, I. D. Abella, and S. R. Hartmann, Phys. Rev. Lett. 13, 567 (1964).
[24]C. A. Hutchison Jr., Marvin D. Kemple, and Y.-T. Yen, Phys. Rev. Lett. 33, 937 (1974).
[25]H. Y. Carr and E. M. Purcell, Phys. Rev. 94, 630 (1954).
[26]S. Meiboom and D. Gill, Rev. Sci. Instrum. 29, 688 (1958).
[27]F. G. Brickwedde, H. van Dijk, M. Durieux, J. R. Clement, and J. K. Logan, J. Res. Natl. Bur. Stand. A 64, 1 (1960).
[28]J. H. Anderson and C. A. Hutchison Jr., Phys. Rev. 97, 76 (1955).
[29]L. G. Rowan, E. L. Hahn, and W. B. Mims, Phys. Rev. 137, A61 (1965).
[30]J. R. Klauder and P. W. Anderson, Phys. Rev. 125, 912 (1962).
[31]B. Herzog and E. L. Hahn, Phys. Rev. 103, 148 (1956).

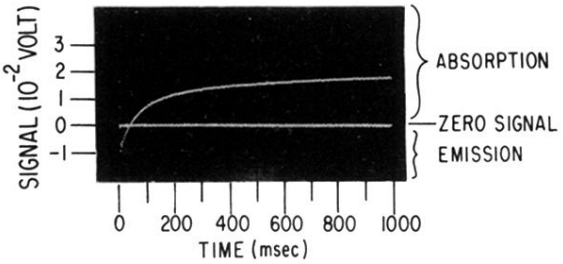

FIG. 2. Oscilloscope trace of magnetic resonance absorption intensity vs time following the termination of a pulse of microwave power. Microwave frequency 1998.02 MHz. Duration of pulse 1.1 μsec. Temperature 1.34 °K. Crystal from boule 2 (see Table I).

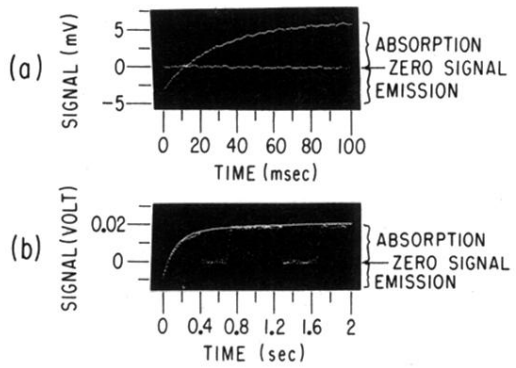

FIG. 4. Oscilloscope trace of magnetic resonance absoprtion intensity vs time following the adiabatic passage of the frequency of the microwave power through resonance. Crystal from boule 3 (see Table I). Temperature (a) 4.210 °K, (b) 1.31 °K.

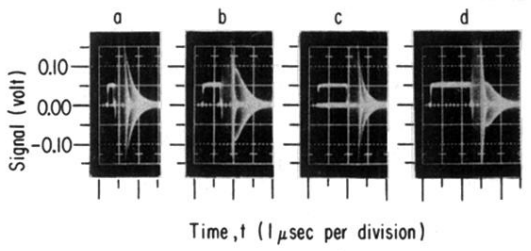

FIG. 5. Oscilloscope traces of intensities of microwave radiation generated by crystal after termination of single pulses of microwave power vs time. Microwave frequency 1998.02 MHz. Temperature 4.21 °K. Crystal from boule 2 (see Table I). Pulse: a, $\frac{1}{2}\pi$; b, $\frac{3}{2}\pi$; c, $\frac{5}{2}\pi$; d, $\frac{7}{2}\pi$.

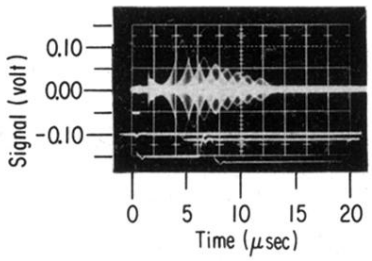

FIG. 6. Multiple-exposure photograph of oscilloscope traces of intensities of microwave echoes generated by crystal, following $\frac{1}{2}\pi, \pi$ pulse pairs of microwave power with varying intervals τ vs time. (The oscilloscope was triggered ~0.11 μsec before the initiation of the second pulse.) Microwave frequency 1998.02 MHz. Temperature 4.22 °K. Crystal from boule 2 (see Table I).

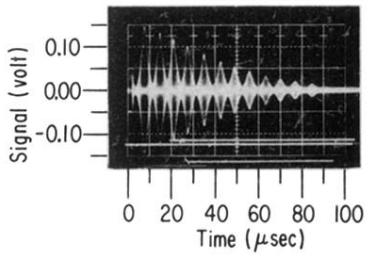

FIG. 7. Multiple-exposure photograph of oscilloscope traces of intensities of microwave echoes generated by crystal, following $\frac{1}{2}\pi, \pi$ pulse pairs of microwave power with varying intervals τ vs time. (The oscilloscope was triggered ~0.11 μsec before the initiation of the second pulse.) Microwave frequency 1998.02 MHz. Temperature 4.21 °K. Crystal from boule 1 (see Table I).

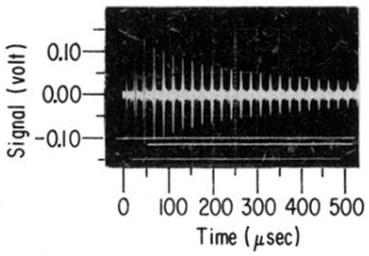

FIG. 8. Oscilloscope trace of intensities of microwave echoes generated by crystal following the pulses of a Carr, Purcell, Meiboom, and Gill sequence vs time. (The oscilloscope was triggered at the beginning of the first pulse.) Microwave frequency 1998.02 MHz. Pulse interval 9.6 μsec. Temperature 4.21 °K. Crystal from boule 1 (see Table I).